RESEARCH ARTICLE | NOVEMBER 17 2025

Crystalline scintillation materials of the aluminum–gallium family to equip light satellites with neutron detectors

M. Korzhik ✉ ⓘ ; V. Bogomolov; A. Bondarau ⓘ ; E. Borisevich ⓘ ; O. Buzanov; A. Iyudin; P. Karpyuk;
I. Komendo; I. Lagutskiy ⓘ ; K. Okhotnikova ⓘ ; V. Smyslova ⓘ ; S. Svertilov; A. Vasil'ev ⓘ ; V. Vasiliev ⓘ

Check for updates

View Online   Export Citation

Crystalline scintillation materials of the aluminum–gallium family to equip light satellites with neutron detectors

M. Korzhik,[1,2,a] V. Bogomolov,[3,4] A. Bondarau,[5] E. Borisevich,[2] O. Buzanov,[6] A. Iyudin,[3,4] P. Karpyuk,[1]
I. Komendo,[1] I. Lagutskiy,[7] K. Okhotnikova,[5] V. Smyslova,[1] S. Svertilov,[3,4] A. Vasil'ev,[4] and V. Vasiliev[5]

AFFILIATIONS

[1]NRC "Kurchatov Institute," Moscow, Russia
[2]Institute for Nuclear Problems, Belarus State University, Minsk, Belarus
[3]Physics Department, M.V. Lomonosov Moscow State University, Moscow 119991, Russia
[4]D.V. Skobeltsyn Institute of Nuclear Physics, M.V. Lomonosov Moscow State University, Moscow 119991, Russia
[5]Physical Departimen, Belarus State University, Minsk, Belarus
[6]FOMOS MATERIALS, Moscow, Russia
[7]ATOMTEX SPE, Minsk, Belarus

[a]Author to whom correspondence should be addressed: korjikmikhail@gmail.com

ABSTRACT

Lightweight satellites, which monitor different kinds of ionizing radiation in the Earth's orbits, need lightweight detectors as well. For the first time, the detecting capabilities of new high light yield and fast scintillation materials of garnet structure, $Gd_3Al_{2.5}Ga_{2.5}O_{12}$:Ce,Mg (GAGG:Ce,Mg-HL) and $Y_3Al_{2.5}Ga_{2.5}O_{12}$:Ce,Mg (YAGG:Ce,Mg-HL), which were produced in the form of single crystals and ceramics, have been evaluated to construct miniature detectors of neutrons. Scintillators have a light yield over 45 000 ph/MeV; at that, Gd-less material has twice as short scintillation kinetics. Both achievements were obtained due to the combined variation in the Al/Ga ratio and Mg doping of the materials. When detecting thermal and epithermal neutrons, YAGG:Ce,Mg-HL will be used as a γ-ray monitor to extract background from the data acquired by GAGG:Ce,Mg-HL. Fast neutrons will produce an identical set of charged secondaries in the materials, which can be distinguished by the pulse shape discrimination method. This finding allows us to construct a miniature detector of neutrons to equip even nanosatellites to monitor space and the secondary neutrons.

I. INTRODUCTION

Neutron flux measuring in space has remained a challenging task for the last decades. The detector design is always a compromise between the limitation on the total launched weight and the weight of either the thermal or background detector shielding, which ensures an acceptable count rate of useful signals. Therefore, searching for new materials that provide the creation of lightweight satellite-based detectors is of particular interest. It is due to the need for a better understanding of the influence of the neutron flux in near-Earth and interplanetary space on the spheres of human activity. In general, cosmic radiation consists of Galactic Cosmic Rays (GCRs) and Solar Energetic Particles (SEPs) and their associated secondary particles.[1] GCRs are predominantly high-energy protons[2] with an average flux of ∼4 protons/cm²/s and with a wide distribution of energies. They produce a shower of secondary particles when interacting with the space craft materials, planet atmosphere, or planet surface.[3] Secondaries include neutrons with energy up to 100 MeV. In addition, x- and γ rays are produced as a result of inelastic scattering and radiation capture of neutrons. The amount of GCRs reaching the Earth's atmosphere depends on the strength of the magnetic field and the energy of the GCR particles.[4] SEPs include charged particles (protons and alpha-particles) and

uncharged particles (neutrons and neutrinos) with a wide range of energies from tens of keV to GeV and intensities.[5,6] The processes described above are a known radiation hazard for space-operating satellites and the health of spacecraft crews, in particular, for missions outside of the Earth.[7,8] Worth noting, the contribution of cosmic radiation to the formation of climatic conditions in the Earth's atmosphere is not completely understood. Charged particles of the solar wind are mostly reflected by the Earth's own magnetic field, and only a portion of them reach the upper layers of the atmosphere, stimulating the redistribution of ions and changes in Earth's ozone layer near the poles.[9–11] However, uncharged particles, such as gamma rays or neutrons, penetrate independently of the Earth's magnetic field, leading to a significant restructuring of the chemical composition and physical properties of the atmosphere. A possible correlation was suggested between the intensity of cosmic rays produced by solar cycle activity and the formation of cloud condensation nuclei in the atmosphere.[12–14] Ultimately, a conclusion was drawn about the new particle formation (NPF), a process called nucleation, and it was proven that about half of all cloud condensation nuclei are formed through NPF.[15–18] Neutrons in the atmosphere can experience elastic and inelastic collisions, as well as undergo nuclear reactions.[19–21] In the case of the first two types of interactions, one can observe an amplification of effects characteristic of γ rays. Apparently, the most prominent in the atmosphere are (n, γ) and (n, p) reactions with the nuclei of ^{14}N and ^{16}O, as well as the formation of deuterium and tritium. As with inelastic collisions, (n, γ) reactions are capable of only enhancing the effects characteristic of γ rays, altering the physical properties of the atmosphere, increasing the production of cloud condensation nuclei, and, consequently, forming a temperature gradient in air masses. SEPs contain some fraction of relativistic neutrons[22–24] because their flux is limited by the short lifetime of a free neutron.[25]

Scintillator-based detecting systems are sufficiently effective in the field of monitoring under conditions of highly intense radiation fields.[26,27] Space physics makes use of scintillators in two different locations: low-orbit satellites and space or interplanetary missions. The low-orbit satellites are shielded by the Earth's magnetic field; therefore, the requirement for radiation hardness of the scintillation material can be significantly reduced. However, in the interplanetary space, the solar wind from charged particles strongly influences the detection requirements of the scintillation materials. For these missions, high radiation hardness to ionizing radiation and low levels of induced radioactivity of detecting materials are required.[28] Another requirement is little influence of the temperature changes on the response of the scintillation detector.

Recently, it was demonstrated that cerium-doped gadolinium aluminum gallium garnet (GAGG:Ce) has an excellent response profile change vs temperature in a wide range, both in light yield and scintillation kinetics.[29] It resolves at least the thermo shielding problem and, therefore, pushes forward an interest in the material to operate on satellites.[30–32] Moreover, GAGG:Ce is non-hygroscopic, radiation hard, bright, fast and, dense, and it has minor light output degradation with accumulated irradiation dose.[27] Gd containing GAGG:Ce effectively absorbs thermal neutrons following the prompt emission of x- and γ rays; therefore, it is also suitable for neutron detection.[33–36] Moreover, the capability of the separation of signals

of the secondaries created by fast and slow neutrons in the scintillator was confirmed as well.[37,38] To reduce the radiation background at the detector on the satellite, the addition of lead and copper shielding may solve the problem,[39] but it is practically not acceptable for nanosatellites.

GAGG:Ce has a high light yield, and it is under industrial production.[40,41] To arrange separate counting of the background events, this material can be combined in a phoswitch detecting element[42] or coupled to separate photosensors with another scintillator, a background monitor, having near-identical response to the high-energy neutrons. The most convenient for this purpose are the garnet Gd-less scintillation materials; however, typically, they have a light yield twice as small as GAGG:Ce.[43] Recently, a high-light yield, neutron-insensitive $Y_3Al_{2.5}Ga_{2.5}O_{12}$:Ce,Mg scintillation material was developed.[44] To keep a similar response to the fast neutrons, we also changed the Al/Ga ratio in GAGG:Ce from 2/3 to 2.5/2.5. The characterization of these materials and the capabilities to utilize them to detect neutrons and discriminate the background are the focus of the article.

II. EXPERIMENTAL METHODS AND DISCUSSION

A. Samples

The family of aluminum–gallium garnet structure compounds is quite flexible to use different methods to obtain them with variation in the cationic composition in a crystalline form. Studied high light yield (HL) GAGG:Ce,Mg-HL crystals have been grown by the Czochralski method from an iridium crucible from the raw material having an Al/Ga ratio of 2.5/2.5. This technique is well developed to produce large-diameter GAGG:Ce single crystals.[40,41] A change in the Al/Ga ratio from 2/3 to 2.5/2.5 in the raw material composition increases the temperature of crystallization; therefore, a neutral atmosphere containing a certain amount (∼3 vol. %) of oxygen was used in a crystallization chamber to avoid gallium evaporation.[45] In addition, we paid attention to the homogenization of the initial charge having a garnet structure. A full incorporation of Ga in the lattice of the initial powder guaranteed a low evaporation of gallium from the filled crucible, when the charge was heated to obtain the melt. The concentration of Ce in the raw material varied from 800 to 2000 ppm. Magnesium codoping at the level of 20 ppm was used to suppress the phosphorescence. When yttrium was used instead of gadolinium in the matrices, the ceramic route was used to obtain YAGG:Ce,Mg-HL scintillation plates. The technology of transparent ceramic material production is described elsewhere.[46] Ce concentration used to be 3000 ppm. The key point of the production route is the nanostructuring of the raw material. It promotes solving the problem of gallium leakage during the high-temperature synthesis of ceramics. Nanostructuring is achieved by producing the precursor by the inverse coprecipitation method. Its utilization ensures minimal amounts of elements that have not passed into the sediment and guarantees the preservation of the specified composition, as well as the reproducibility of syntheses. Moreover, nanostructuring allows increasing the rate of compaction of the raw material during sintering due to the high reactivity of the precursor particles with a developed surface. Preheated powder was used to obtain green bodies. X-ray diffraction data show that

during heat treatment at 900 °C for 10 h, the cubic phase of garnet with the space group Ia3d becomes dominant, and the phase with the hexagonal perovskite structure (space group P63/mm c) is not observed.

Single crystalline and ceramics samples, which were made for the characterization of the scintillation parameters and measurements of the response to different sources of ionizing radiation, are shown in Fig. 1. GAGG:Ce,Mg-HL samples were produced in the form of elements with dimensions of $1 \times 1 \times 2$, $1 \times 1 \times 1$, and $1.4 \times 1.4 \times 1$–0.02 cm^3, whereas YAGG:Ce,Mg-HL was produced in the form of circle plates allowing the production of elements with dimensions $1.2 \times 1.2 \times 1 \times 0.1$ cm^3.

B. Characterization of samples

The measurements with neutrons were performed at ATOMTEX certified dosimetry facilities, including ^{238}PuBe- and ^{137}Cs-based benches. A ^{238}PuBe source with a 20 cm long plastic moderator was used to obtain thermal neutrons. Photoluminescence spectra of the samples were recorded using a Fluorat-02-PANORAMA spectro-fluorimeter at the excitation in the lowest Ce^{3+} ion absorption transition 4f^1-4f^{1}5d$_1$. Spectra were found to be identical to those that were measured at x-ray excitation. The light yield (LY) was evaluated with a CAMAC-based data acquisition system with an integration time of 7 μs and an R329 (Hamamatsu) photomultiplier tube (PMT). A CsI (Tl) scintillator with a light yield of 54 000 ph/MeV and a diameter and height of 1 in. was used as a reference sample. The light yield non-proportionality was measured with the same PMT with readout by a DRS-4 digitizer, providing digitization of each scintillation pulse in a time interval of 1.5 μs. Laboratory isotope sources ^{241}Am (59.6 keV), ^{137}Cs (184, 662 keV), and ^{22}Na (170, 511, and 1022 keV) were used for this purpose. Scintillation kinetics was measured by
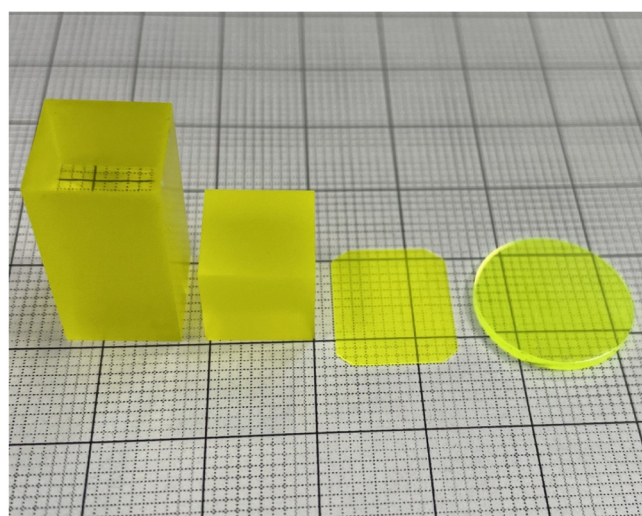

FIG. 1. Detecting elements used for the evaluation of detecting properties. From left to right: two single crystalline and one ceramic GAGG:Ce,Mg-HL; the last in the line is ceramic YAGG:Ce,Mg-HL.

the method of delayed coincidences with a Photonis XP2020 PMT in both channels. All measurements were performed at room temperature.

C. Scintillation properties

Figure 2 summarizes the scintillation properties of GAGG:Ce, Mg-HL and YAGG:Ce,Mg-HL scintillation materials having an Al/Ga ratio of 2.5/2.5 in composition. Figure 2(c) shows a change in the scintillation kinetics of the GAGG:Ce,Mg-HL samples when the Ce concentration was increased from 800 (curve 1) to 2000 ppm (curve 2). Obviously, reducing the activator concentration of the crystal affects the kinetics curve in a stronger way in comparison to ordinary GAGG:Ce. Kinetic curves have been acquired with different statistics for better perception on the panel.

Taking into account the spectral sensitivity of the PMT to the scintillation spectrum, the light output for the studied samples was estimated to be 45 000 and 51 000 ± 1000 ph/MeV for YAGG:Ce, Mg-HL and GAGG:Ce,Mg-HL, respectively. We did not make special efforts to obtain the highest energy resolution. However, when a silicon photomultiplier is used, the GAGG scintillator, with a similar or even lower LY, exhibits energy resolution below 7% for the energy 511 keV.[47] The scintillation kinetics of GAGG:Ce, Mg-HL (Ce 800 ppm) were approximated with two exponents with decay constants 76 (30%) and 380 (70%), whereas for the sample having 2000 ppm of Ce, the best fit was achieved for the same number of exponents with decay constants 48 (60%) and 209 (40%) ns. The YAGG:Ce,Mg-HL kinetics was characterized with 32 (55%) and 64 (44%) ns decay constants. The effective decay constants were estimated as $\sum_i \tau_i f_i$, where f_i is a fraction of the component with decay constant τ_i. Calculated values are 290 ± 5, 110 ± 5, and 46 ± 5 ns, correspondingly. Both materials demonstrated a drop of the output at the level of 10% in the energy range of 59.6–662 keV.

D. Response to neutrons

Figure 3(a) depicts the response of the GAGG:Ce,Mg-HL sample with dimensions of $1 \times 1 \times 2$ cm^3 to neutrons from the ^{238}PuBe source, the natural background with a dose rate of 0.1 mkSv/h, and 662 keV γ rays from the ^{137}Cs source with a dose rate of 7 mkSv/h. The acquisition time was chosen to be 300 s; the neutron flux at a measurement point was 121.6 n/sm$^2 \times$ s. Based on the measurements mentioned above, Fig. 3(b) is obtained. It presents the dependence of the relative counting efficiency of the $1 \times 1 \times 2$ cm^3 GAGG:Ce,Mg-HL sample on neutrons from the ^{238}PuBe source with a 20 cm thick moderator vs the energy range in which detector counts are acquired.

One can state that the efficiency reaches 40% of the total value in the energy range of the secondaries up to 100 keV. Moreover, it comes to 90% in the energy range limited by annihilation γ rays.

Details of the spectra of the response to neutrons are described elsewhere.[35–38] Note that efficiency reaches 40% when pulsed and counted in the energy range up to 100 keV. Figure 4 shows the response of the GAGG:Ce,Mg-HL detecting element with dimensions of $1.2 \times 1.2 \times 0.02$ cm^3 to the thermal neutrons of the ^{238}PuBe source.

The peak at ~86 keV dominates in the spectrum. It is caused by the prompt ionizing radiation accompanying neutron capture
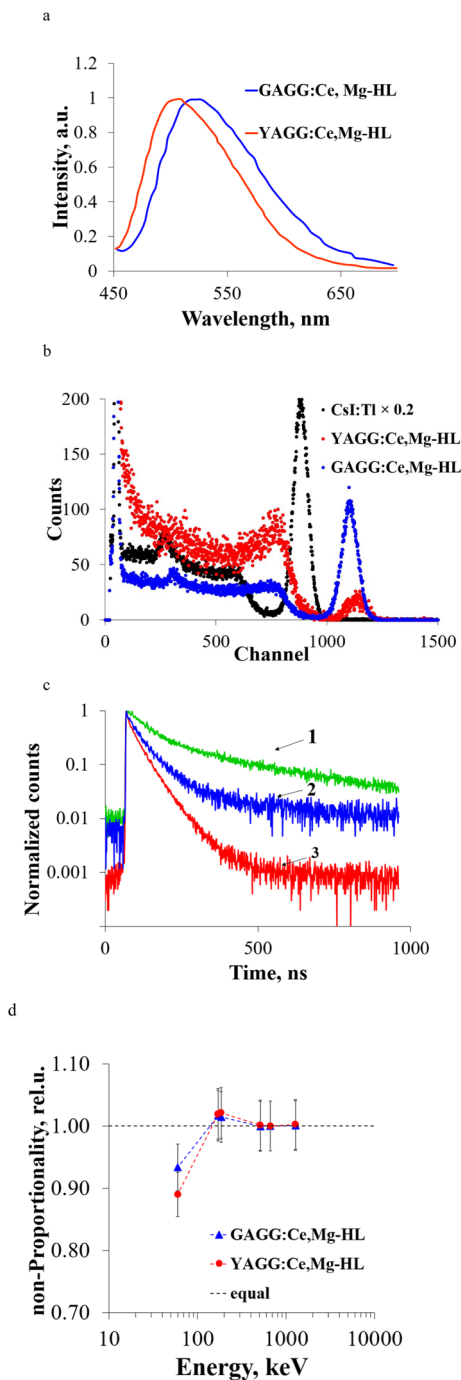
FIG. 2. Comparison of the scintillation properties of $Gd_3Al_{2.5}Ga_{2.5}O_{12}$:Ce,Mg and $Y_3Al_{2.5}Ga_{2.5}O_{12}$:Ce,Mg crystalline scintillation materials: (a) luminescence under excitation in the first Ce^{3+} $4f^1$-$4f^0$$5d_1$ transition; (b) pulse height spectra of $1 \times 1 \times 1$ cm^3 GAGG:Ce,Mg-HL and $1.2 \times 1.2 \times 0.1$ cm^3 YAGG:Ce,Mg-HL samples in comparison to a reference CsI(Tl) scintillator; (c) scintillation kinetics: 1- GAGG:Ce,Mg-HL(800 ppm), 2- GAGG:Ce,Mg-HL (2000 ppm), and 3- YAGG: Ce,Mg-HL; (d) non-proportionality of the responses to γ rays.
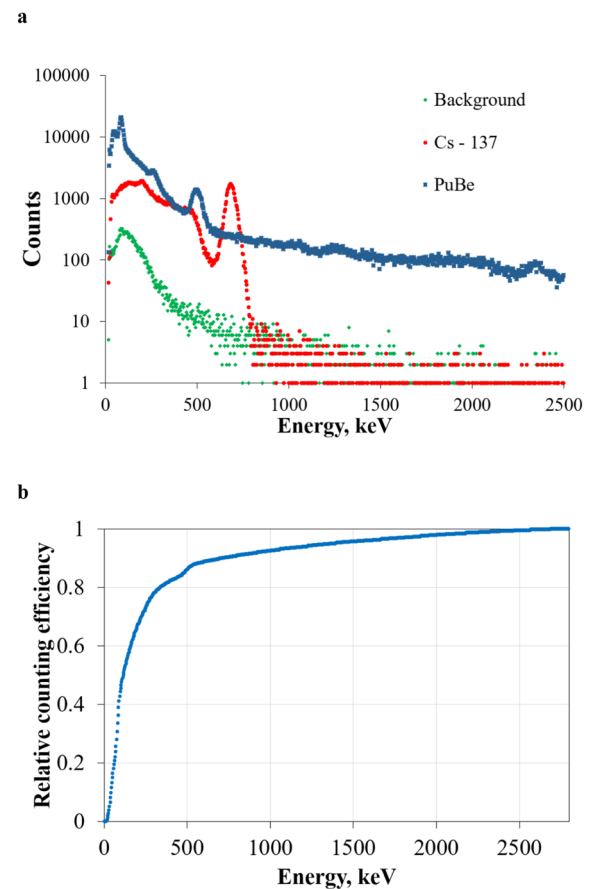

FIG. 3. Response of the GAGG:Ce,Mg-HL scintillation element with dimensions $1 \times 1 \times 2$ cm^3 to neutrons from the ^{238}PuBe source with a 20 cm thick plastic, natural background, and 662 keV γ rays from the ^{137}Cs source with a dose of 7 mkSv/h (a); calculated dependence of the relative counting efficiency of the $1 \times 1 \times 2$ cm^3 GAGG:Ce,Mg-HL sample to neutrons from the ^{238}PuBe source vs energy range (b).

reactions by gadolinium isotope nuclei (^{155}Gd and ^{157}Gd). The peak is created by the energy release in the scintillator by conversion electrons and x rays.

E. Discrimination of γ rays when detecting with coupled YAGG:Ce,Mg-HL and GAGG:Ce,Mg-HL elements

Figure 5 demonstrates the 2D histograms of pulse shape discriminated (PSD) pulses of the ^{241}Am (a) and ^{137}Cs(b) sources measured with a $1.2 \times 1.2 \times 0.1$ cm^3 YAGG:Ce,Mg-HL sample and a $1.2 \times 1.2 \times 0.02$ cm^3 GAGG:Ce,Mg-HL (concentration of Ce 2000 ppm) plate arranged in phoswich and read with the PMT. The latter plate was coupled to the PMT window, whereas the lighter YAGG garnet was on the top of the assembly. Due to the absorption of the γ rays by YAGG, the statistics measured with GAGG are few in number. Nevertheless, due to a difference
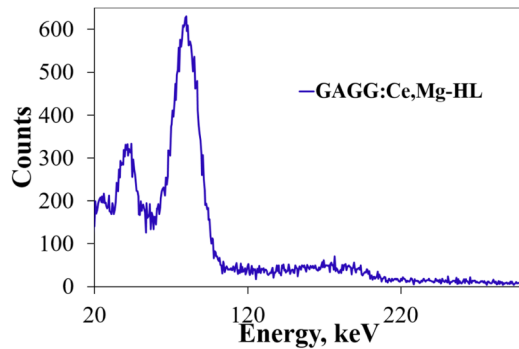
FIG. 4. Response of $1.2 \times 1.2 \times 0.02 \ cm^3$ GAGG:Ce,Mg-HL to the ^{238}PuBe source with a 20 cm long plastic moderator mounted in between the detector and the source. Neutron flux at the point of measurement was 78 n/cm², acquisition time was 1800 s, and the natural background measured in the same position without source was extracted.

in the scintillation kinetics, events in both plates are satisfactorily separated. Discrimination would be even better if GAGG:Ce, Mg-HL with a concentration of Ce of 800 ppm or even less were utilized.

To construct the PSD spectrogram, the following time windows were used: "short" $Q_s \sim 100$ ns and "long" $Q_l \sim 900$ ns from the peak of the scintillation pulse. The scintillation charge of each pulse from the PMT output was calculated as the sum of the amplitude values in each sampling interval. For each pulse recorded by the ADC, a PSD parameter was calculated as follows:

$$PSD = 1 - Q_s/Q_l.$$

The parameter FoM (Figure of Merit) was used as a criterion for signal discrimination.[48] FoM ~ 1.24 was obtained for measurements with ^{137}Cs source, and ~ 0.63—for measurements with ^{241}Am source.

The obtained results confirm that the gadolinium–aluminum–gallium garnet is very effective for detecting the thermal neutrons. It is also quite effective for recording fast and high-energy neutrons, which was confirmed for the particles with an energy of more than 10 MeV when charged secondaries are formed in the scintillator material.[37,38] The response to secondaries is perfectly separated from γ rays in the spectrum using the PSD. Note the importance of the similar composition of light atoms (O, Al, Ga) in YAGG:Ce,Mg-HL and YAGG:Ce,Mg-HL. Their nuclei are responsible for interaction with fast neutrons. Such neutrons, even
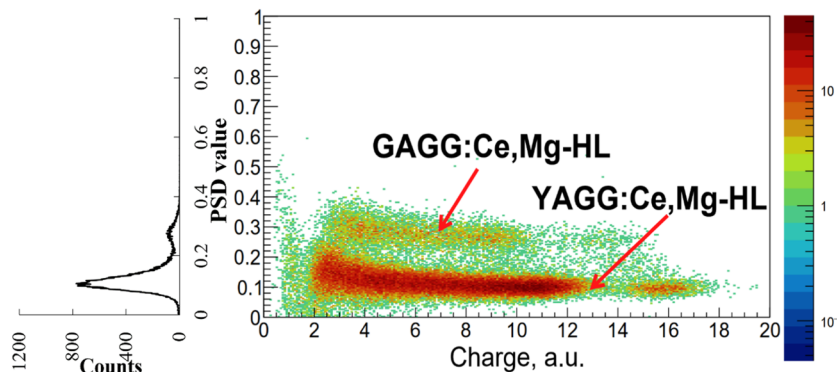
a
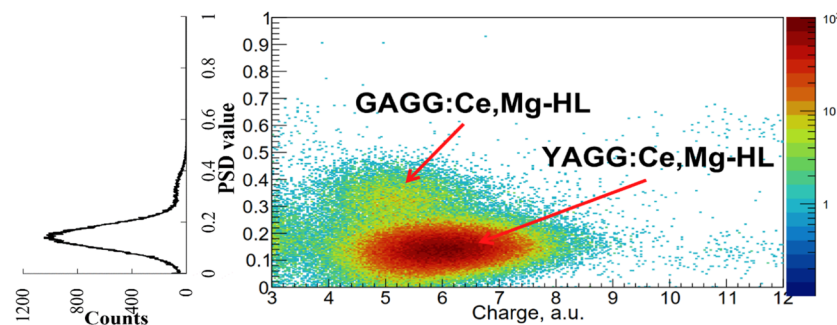
b

FIG. 5. 2D histograms of the PSD value vs integral (right) and figures of merit (left) measured with ^{241}Am (a) and ^{137}Cs (b) with $1.2 \times 1.2 \times 0.1 \ cm^3$ YAGG:Ce, Mg-HL and $1.2 \times 1.2 \times 0.02 \ cm^3$ GAGG:Ce,Mg-HL plates arranged in phoswich. YAGG:Ce,Mg-HL was at the top of the assembly.

when interacting with the YAGG:Ce,Mg-HL X/γ-monitor, will be reliably discriminated due to the difference in scintillation kinetics. Moreover, as seen from Fig. 5, background low-energy γ-quanta overlapping the main peak in the vicinity of 80 keV in the neutron-sensitive detecting element may be discriminated as well. These detector capabilities allow to significantly reduce the mass and volume of the detector element absorption shielding, while both the neutron-sensitive and insensitive elements can be read by one photodetector.

F. Future optimization of the Gd content in the GAGG:Ce,Mg-HL

An important issue is the size of the detector's neutron-sensitive element. Figure 6 depicts the results of modeling by the GEANT 4 package and shows the attenuation of the neutron flux of different energies of the scintillation material $Gd_xY_{3-x}Al_{2.5}Ga_{2.5}O_{12}$ depending on the gadolinium content x in the matrix. Since the absorption cross section of thermal neutrons by a natural mixture of gadolinium atoms is ~49 000 barns,[33] the close to full absorption of the neutrons occurs in a matrix containing only gadolinium, in a layer less than 50 μm. Therefore, the use of bulk elements for such a purpose is not optimal; the detector element will effectively accumulate events of interaction with the high-energy component of the γ-background as seen from the comparison of data in Figs. 3 and 4. Dilution of the matrix with yttrium can lead to an increase in the sensitive volume in the detector element: When the content is reduced by a factor of 30 to x = 0.1, the effective working layer increases to a value of slightly more than 2 mm.

Worth noting, the development of the scintillation material $Y_3Al_{2.5}Ga_{2.5}O_{12}$:Ce,Mg with a high scintillation yield ensures that with a decrease in the gadolinium content to x = 0.1 or less, the scintillation yield of the material more likely will keep as high. For epithermal and fast neutrons, due to a decrease in the cross section by Gd nuclei, the thickness of the layer effectively absorbing neutrons increases significantly. Therefore, the detecting elements with a volume of several cubic cm are intended specifically for recording epithermal and fast neutrons, while thin elements would be enough to provide high efficiency for recording the thermal neutrons.
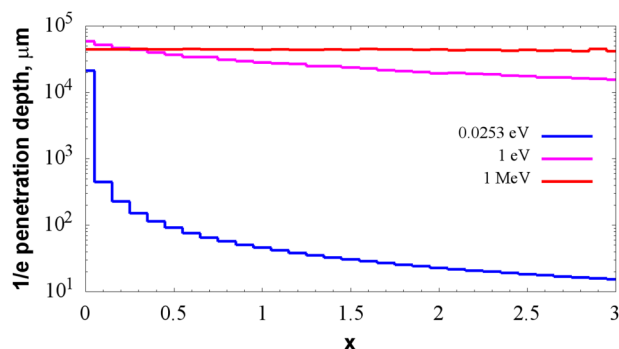

FIG. 6. The modeled attenuation length by a factor of 1/e of the flux of the neutrons of different energies (indicated) for the scintillation material $Gd_xY_{3-x}Al_{2.5}Ga_{2.5}O_{12}$ depending on the gadolinium content x in the matrix.

III. CONCLUSIONS

$Gd_3Al_{2.5}Ga_{2.5}O_{12}$:Ce,Mg and $Y_3Al_{2.5}Ga_{2.5}O_{12}$:Ce,Mg crystalline scintillation materials with high scintillation yield and their decay constants differing by a factor of 2 or even more have been produced by different techniques, including crystal growth by the Czochralski method and sintering of the ceramics. Materials were evaluated to detect neutrons and to discriminate γ rays of different energies. Data obtained confirm the capability to create miniature neutron detectors that operate over a wide energy range and have a low weight and volume. A gadolinium-less scintillator will be used to accumulate events of either x-ray or γ-ray background for its subsequent subtraction from the data accumulated by a gadolinium-containing detector element. Both detecting elements will be able to detect high-energy neutrons, and their responses will be reliably separated by scintillation pulse shape as well. This affords avoiding the need for using bulky passive protection from γ rays, which makes it possible to use such detectors even on small satellites and nanosatellites.

AUTHOR DECLARATIONS

Conflict of Interest

The authors have no conflicts to disclose.

Author Contributions

M. Korzhik: Writing – original draft (equal). **V. Bogomolov:** Investigation (equal). **A. Bondarau:** Data curation (equal). **E. Borisevich:** Data curation (equal). **O. Buzanov:** Investigation (equal). **A. Iyudin:** Conceptualization (equal). **P. Karpyuk:** Investigation (equal). **I. Komendo:** Conceptualization (equal). **I. Lagutskiy:** Validation (equal). **K. Okhotnikova:** Methodology (equal). **V. Smyslova:** Visualization (equal). **S. Svertilov:** Methodology (equal). **A. Vasil'ev:** Writing – review & editing (equal). **V. Vasiliev:** Formal analysis (equal).

DATA AVAILABILITY

The data that support the findings of this study are available within the article.

REFERENCES

[1]J. D. Haigh, "Solar terrestrial interactions," in *Encyclopedia of Atmospheric Sciences* (Elsevier, 2003), pp. 2072–2078.

[2]See https://home.cern/science/physics/cosmic-rays-particles-outer-space for "Cosmic rays: Particles from outer space, CERN" (accessed 2 October 2025).

[3]L.-A. A. McFadden, P. R. Weissman, and T. V. Johnson, *Encyclopedia of the Solar System*, 2nd ed. (Academic, Amsterdam, 2007).

[4]S. A. Elias, *Encyclopedia of Quaternary Science*, 1st ed. (Elsevier, Amsterdam, 2006).

[5]T. P. Dachev, J. V. Semkova, B. T. Tomov, Y. N. Matviichuk, P. G. Dimitrov, R. T. Koleva, S. Malchev, N. G. Bankov, V. A. Shurshakov, V. V. Benghin, E. N. Yarmanova, O. A. Ivanova, D.-P. Häder, M. Lebert, M. T. Schuster, G. Reitz, G. Horneck, Y. Uchihori, H. Kitamura, O. Ploc, J. Cubancak, and I. Nikolaev, "Overview of the liulin type instruments for space radiation measurement and their scientific results," Life Sci. Space Res. **4**, 92–114 (2015).

[6]K. Whitman, R. Egeland, I. G. Richardson, C. Allison, P. Quinn, J. Barzilla, I. Kitiashvili, V. Sadykov, H. M. Bain, M. Dierckxsens, M. L. Mays, T. Tadesse, K. T. Lee, E. Semones *et al.*, "Review of solar energetic particle prediction models," Adv. Space Res. **72**(12), 5161–5242 (2023).

[7]T. Hutton, A. Buffler, M. Kidson, E. Fairall, and R. Babut, "Neutron spectrometry in space and aviation with a compact scintillator-based detector," Appl. Radiat. Isot. **225**, 111917 (2025).

[8]*Extreme Events in Geospace* (Elsevier, 2018).

[9]A. A. Krivolutsky, A. A. Kuminov, T. Y. V'yushkova, S. N. Kuznetsov, and I. N. Myagkova, "Changes in the Earth's ozonosphere due to ionization of high-latitude atmosphere by solar protons in October, 2003," Cosmic Res. **42**(6), 626–635 (2004).

[10]C. H. Jackman, R. D. McPeters, G. J. Labow, E. L. Fleming, C. J. Praderas, and J. M. Russell, "Northern hemisphere atmospheric effects due to the July 2000 solar proton event," Geophys. Res. Lett. **28**(15), 2883–2886, https://doi.org/10.1029/2001gl013221 (2001).

[11]A. Krivolutsky, A. Kuminov, and T. Vyushkova, "Ionization of the atmosphere caused by solar protons and its influence on ozonosphere of the Earth during 1994–2003," J. Atmos. Sol.-Terr. Phys. **67**(1–2), 105–117 (2005).

[12]K. S. Carslaw, R. G. Harrison, and J. Kirkby, "Cosmic rays, clouds, and climate," Science **298**(5599), 1732–1737 (2002).

[13]J. Kirkby, "Cosmic rays and climate," Surv. Geophys. **28**(5–6), 333–375, https://doi.org/10.1007/s10712-008-9030-6 (2007).

[14]H. Svensmark and E. Friis-Christensen, "Variation of cosmic ray flux and global cloud coverage—a missing link in solar-climate relationships," J. Atmos. Sol.-Terr. Phys. **59**(11), 1225–1232 (1997).

[15]C. Rose, K. Sellegri, I. Moreno, F. Velarde, M. Ramonet, K. Weinhold, R. Krejci, M. Andrade, A. Wiedensohler, P. Ginot, and P. Laj, "CCN production by new particle formation in the free troposphere," Atmos. Chem. Phys. **17**(2), 1529–1541 (2017).

[16]J. F. Ormes, "Cosmic rays and climate," Adv. Space Res. **62**(10), 2880–2891 (2018).

[17]Y. Chapanov and V. Gorshkov, "Solar activity and cosmic ray influence on the climate," Geomagn. Aeron. **59**(7), 942–949, https://doi.org/10.1134/s0016793219070090 (2019).

[18]J. Kirkby, A. Amorim, U. Baltensperger, K. S. Carslaw, J. Christoudias, J. Curtius, N. M. Donahue, I. E. Haddad, R. C. Flagan, H. Gordon, A. Hansel, H. Harder, H. Junninen, M. Kulmala, A. Kürten, A. Laaksonen, K. Lehtipalo, J. Lelieveld, O. Möhler, I. Riipinen, F. Stratmann, A. Tomé, A. Virtanen, R. Volkamer, P. M. Winkler, and D. R. Worsnop, "Atmospheric new particle formation from the CERN CLOUD experiment," Nat. Geosci. **16**(11), 948–957 (2023).

[19]P. Goldhagen, "Cosmic-ray neutrons on the ground and in the atmosphere," MRS Bull. **28**(2), 131–135 (2003).

[20]R. C. Haymes, "Terrestrial and solar neutrons," Rev. Geophys. **3**(3), 345–364, https://doi.org/10.1029/rg003i003p00345 (1965).

[21]S. Shibata, "Propagation of solar neutrons through the atmosphere of the Earth," J. Geophys. Res. **99**(A4), 6651–6665, https://doi.org/10.1029/93ja03175 (1994).

[22]R. E. Lingenfelter, E. J. Flamm, E. H. Canfield, and S. Kellman, "High-energy solar neutrons: 2. Flux at the Earth," J. Geophys. Res. **70**(17), 4087–4095, https://doi.org/10.1029/jz070i017p04087 (1965).

[23]R. E. Ligenfelter, E. J. Flamm, E. H. Canfield, and S. Kellman, "High-energy solar neutrons: 1. Production in flares," J. Geophys. Res. **70**(17), 4077–4086, https://doi.org/10.1029/jz070i017p04077 (1965).

[24]E. L. Chupp, "Solar neutron observations and their relation to solar flare acceleration problems," Sol. Phys. **118**(1–2), 137–154 (1988).

[25]A. T. Yue, M. S. Dewey, D. M. Gilliam, G. L. Greene, A. B. Laptev, J. S. Nico, W. M. Snow, and F. E. Wietfeldt, "Improved determination of the neutron lifetime," Phys. Rev. Lett. **111**(22), 222501 (2013).

[26]R.-Y. Zhu, "Ultrafast and radiation hard inorganic scintillators for future HEP experiments," J. Phys.: Conf. Ser. **1162**, 012022 (2019).

[27]P. Lecoq, A. Gektin, and M. Korzhik, *Inorganic Scintillators for Detector Systems* (Springer International Publishing, Cham, 2017).

[28]C. W. Fabjan and H. Schopper, "Particle physics reference library," in *Detectors for Particles and Radiation* (Springer International Publishing, Cham, 2020), Vol. 2. .

[29]M. Kole, K. Wimalasena, R. Gorby, T. Diesel, Z. Greenberg, and F. Kislat, "Low-temperature performance of $Gd_3(Ga, Al)_5O_{12}$:Ce scintillators," arXiv:2508.13844 (2025).

[30]Y. Zhu, S. Qian, Z. Wang, H. Guo, L. Ma, Z. Wang, and Q. Wu, "Scintillation properties of GAGG:Ce ceramic and single crystal," Opt. Mater. **105**, 109964 (2020).

[31]M. Pallu, D. Pailot, E. Bréelle, P. Laurent, J. Carron, F. Lebrun, C. Koumeir, C. Chapron, and K. Biernacki, "Studies of GAGG:Ce scintillators for space missions dedicated to terrestrial gamma-Ray flashes and gamma-ray bursts observation," Nucl. Instrum. Methods Phys. Res., Sect. A **1069**, 169997 (2024).

[32]F. Fuschino, R. Campana, C. Labanti *et al.*, "HERMES: An ultra-wide band X and gamma-ray transient monitor on board a nano-satellite constellation," Nucl. Instrum. Methods Phys. Res., Sect. A **936**, 199–203 (2019).

[33]M. P. Taggart, M. Nakhostin, and P. J. Sellin, "Investigation into the potential of GAGG:Ce as a neutron detector," Nucl. Instrum. Methods Phys. Res., Sect. A **931**, 121–126 (2019).

[34]J. Dumazert, R. Coulon, Q. Lecomte, G. H. V. Bertrand, and M. Hamel, "Gadolinium for neutron detection in current nuclear instrumentation research: A review," Nucl. Instrum. Methods Phys. Res., Sect. A **882**, 53–68 (2018).

[35]A. Fedorov, V. Gurinovich, V. Guzov, G. Dosovitskiy, M. Korzhik, V. Kozhemyakin, A. Lopatik, D. Kozlov, V. Mechinsky, and V. Retivov, "Sensitivity of GAGG based scintillation neutron detector with SiPM readout," Nucl. Eng. Technol. **52**(10), 2306–2312 (2020).

[36]M. Korjik, K.-T. Brinkmann, G. Dosovitskiy, V. Dormenev, A. Fedorov, D. Kozlov, V. Mechinsky, and H.-G. Zaunick, "Compact and effective detector of the fast neutrons on a base of Ce-doped Gd_3 Al_2 Ga_3 O_{12} scintillation crystal," IEEE Trans. Nucl. Sci. **66**(1), 536–540 (2019).

[37]R. S. Woolf, B. F. Phlips, A. L. Hutcheson, L. J. Mitchell, and E. A. Wulf, "High-energy neutron response of the HR-GAGG scintillation crystal," in *2020 IEEE Nuclear Science Symposium and Medical Imaging Conference (NSS/MIC)* (IEEE, Boston, MA, 2020), pp. 1–3.

[38]A. Fedorov, A. Bondarau, A. Dzhurik, V. Bogomolov, A. Iyudin, Y. Kashchuk, V. Mechinsky, S. Obudovsky, S. Svertilov, Y. Wu, D. Yanushevich, and M. Korzhik, "Pulse shape discrimination at the registration of 14.6 MeV neutrons with $Gd_3Al_2Ga_3O_{12}$:Ce/SiPM(PMT) detectors," Nucl. Instrum. Methods Phys. Res., Sect. A **1062**, 169155 (2024).

[39]M. V. Korzhik, A. A. Fedorov, V. A. Mechinskij, G. A. Dosovitskij, and A. E. Dosovitskij, RU 2663683 C1 (2018).

[40]K. Kamada, T. Yanagida, T. Endo, K. Tsutumi, Y. Usuki, M. Nikl, Y. Fujimoto, A. Fukabori, and A. Yoshikawa, "2 inch diameter single crystal growth and scintillation properties of $Ce:Gd_3Al_2Ga_3O_{12}$," J. Cryst. Growth **352**(1), 88–90 (2012).

[41]See https://www.newpiezo.com for "Fomos crystals web site" (accessed 22 August 2025).

[42]S. Min, B. Seo, C. Roh, S. Hong, and J. Cheong, "Phoswich detectors in sensing applications," Sensors **21**(12), 4047 (2021).

[43]W. Chewpraditkul, N. Pattanaboonmee, W. Chewpraditkul, K. Kamada, K. J. Kim, A. Yoshikawa, M. Makowski, M. E. Witkowski, W. Drozdowski, A. Beitlerova, R. Kucerkova, V. Babin, and M. Nikl, "Optical and scintillation

characteristics of $Lu_2Y(Al_{5-x}Ga_x)O_{12}$:Ce,Mg multicomponent garnet crystals," Opt. Mater. **134**, 113186 (2022).

[44]V. Smyslova, A. Bondarau, A. Fedorov, E. Borisevich, I. Lagutskiy, P. Karpuyk, I. Komendo, V. Kalinov, V. Mechinsky, V. Retivov, Y. Talochko, A. Vasil'ev, and M. Korzhik, "New high light yield and fast ceramic scintillator $Y_3Al_{2.5}Ga_{2.5}O_{12}$: Ce, Mg," Photonics **12**(7), 680 (2025).

[45]R. H. Lamoreaux, D. L. Hildenbrand, and L. Brewer, "High-temperature vaporization behavior of oxides II. Oxides of Be, Mg, Ca, Sr, Ba, B, Al, Ga, In, Tl, Si, Ge, Sn, Pb, Zn, Cd, and Hg," J. Phys. Chem. Ref. Data **16**(3), 419–443 (1987).

[46]M. Korzhik, V. Retivov, V. Dubov, V. Ivanov, I. Komendo, D. Lelekova, P. Karpyuk, V. Mechinsky, A. Postupaeva, V. Smyslova, V. Shlegel, I. Shpinkov, and A. Vasil'ev, "Compositional disordering: Nanoscale engineering of advanced crystalline scintillation materials," J. Appl. Phys. **137**(2), 020701 (2025).

[47]G. Tamulaitis, A. Vasil'ev, M. Korzhik, A. Mazzi, A. Gola, S. Nargelas, A. Vaitkevicius, A. Fedorov, and D. Kozlov, "Improvement of the time resolution of radiation detectors based on $Gd_3 Al_2Ga_3O_{12}$ scintillators With SiPM readout," IEEE Trans. Nucl. Sci. **66**(7), 1879 (2019).

[48]M. J. I. Balmer, K. A. A. Gamage, and G. C. Taylor, "Comparative analysis of pulse shape discrimination methods in a 6Li loaded plastic scintillator," Nucl. Instrum. Methods Phys. Res., Sect. A **88**, 146 (2015).

[49]J. Allison, K. Amako, J. Apostolakis *et al.*, "Recent developments in Geant4," Nucl. Instrum. Methods Phys. Res., Sect. A **835**, 186 (2016).

11 December 2025 12:44:33